Available online at www.sciencedirect.com
SCIENCE DIRECT
Sensors and Actuators A 127 (2006) 201–206
SENSORS AND ACTUATORS A PHYSICAL
www.elsevier.com/locate/sna

# Fabrication and characterization of ZnO nanowires based UV photodiodes☆

Lei Luo[a,*], Yanfeng Zhang[b], Samuel S. Mao[b], Liwei Lin[a]

[a] *Berkeley Sensor and Actuator Center, Department of Mechanical Engineering, University of California at Berkeley, 1113 Etcheverry Hall, Berkeley, CA 94720-1740, USA*
[b] *Lawrence Berkeley National Laboratory, Building 70, Berkeley, CA 94720, USA*

Received 2 March 2005; accepted 27 June 2005
Available online 15 August 2005

**Abstract**

A heterojunction of n-type zinc oxide (ZnO) nanowires and p-type silicon has been successfully constructed to demonstrate ultraviolet (UV) photodiodes. The prototype device consists of naturally doped n-type ZnO nanowires grown on top of a (1 0 0) p-silicon substrate by the bottom-up growth process. The diameter of the nanowires is in the range of 70–120 nm, and the length is controlled by the growth time. The isolation is achieved by using spin-on glass (SOG) that also works as the foundation of the top electrode. The current–voltage (*I–V*) characteristics show the typical rectifying behavior of heterojunctions, and the photodiode exhibits response of ~0.07 A/W for UV light (365 nm) under a 20 V reverse bias.


*Keywords:* ZnO nanowires; UV light; Photodiodes

## 1. Introduction

Ultraviolet (UV) photodetectors have a wide range of applications in military and civilian areas, including missile launching detection, flame sensing, UV radiation calibration and monitoring, chemical and biological analysis, optical communications, and astronomical studies [1]. In these applications, high responsivity, fast response time, and good signal-to-noise ratio are common desirable characteristics. Recently, wide-bandgap materials are under intensive studies to improve the responsivity and stability of UV photodetectors [2–4]. Among them, zinc oxide (ZnO) is of great interest due to its strong UV photoresponse, well-established synthesis methods, and the capability of operating at high temperature and in harsh environments [5–7].

One-dimensional (1D) semiconductor nanowires and carbon nanotubes show great potential for next-generation electronic and optoelectronic devices, such as diode logic devices, field-effect transistors, light emitting diodes (LEDs), optoelectronic memory devices, and photodetectors [8–12]. ZnO nanowires with wide-bandgap ($E_g$ ~3.3 eV) characteristics and large surface area to volume ratio should have good UV response to enhance the performance of UV photodiodes. In this paper, a prototype photodiode of n-ZnO nanowires/p-silicon was fabricated and tested under UV illumination. Fig. 1 shows the schematic diagram of the fabricated device. The synthesis of ZnO nanowires was initiated by a thin layer of gold catalyst on top of a p-silicon substrate via the vapor–liquid–solid (VSL) growth mechanism. This process allows direct integration of high quality 1D structures after the growth without introducing damages during the conventional post-processing of nanostructures, such as ultrasonic vibration, fluidic dispersing, and chemical erosions.

☆ A portion of this paper was presented at the18th IEEE Micro Electro Mechanical Systems Conference, Miami, USA, January 30–February 3, 2005.

* Corresponding author. Tel.: +1 510 642 8983.
*E-mail address:* leiluo@me.berkeley.edu (L. Luo).

0924-4247/$ – see front matter © 2005 Elsevier B.V. All rights reserved.
doi:10.1016/j.sna.2005.06.023

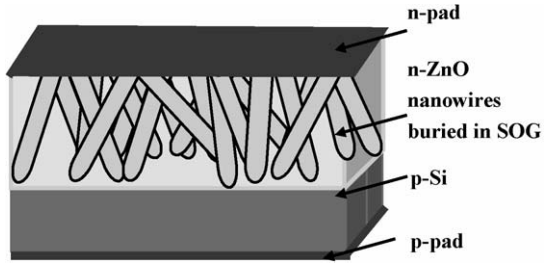


Fig. 1. Schematic diagram of the prototype device consisting of n-ZnO nanowires grown on top of a silicon substrate.

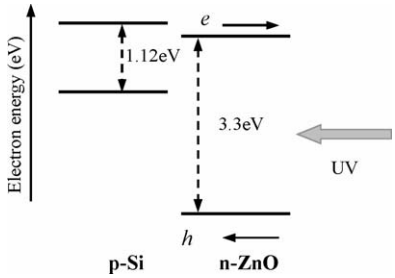


Fig. 2. Schematic energy band diagram of the n-ZnO nanowires/p-silicon structure; electron–hole pairs generated under UV illumination and separated by the electric field inside ZnO nanowires under reverse bias.

## 2. Operation principle

Photodiodes are light-sensitive devices used to detect optical signals through electronic processes, and generally work under photovoltaic or photoconductive mode. The operation involves three steps: (1) carrier generation by absorption of the incident light, of which the photon energy is higher than the bandgap of device materials; (2) carrier transport; and (3) interaction of current with the external circuit to provide the output signal. The maximum wavelength $\lambda_{max}$ of the light that can generate electrons and holes is found as [13]:

$$\lambda_{max} = \frac{hc}{E_g} \tag{1}$$

where $h$ is the Planck's constant; $c$, the velocity of light; and $E_g$ is the bandgap of the semiconductor material. This paper presents devices operating under reverse bias for the photoconductive mode in order to reduce the heterojunction capacitance and the loss of carriers due to a larger depletion width. The depletion width $x_D$ inside the n-type material is expressed as [14]:

$$x_D = \left[\frac{2N_A\varepsilon_D\varepsilon_A(V_{bi} - V)}{qN_D(N_D\varepsilon_D + N_A\varepsilon_A)}\right]^{1/2} \tag{2}$$

where $N_D$, $N_A$, and $\varepsilon_D$, $\varepsilon_A$ are the doping levels and dielectric constants of the n-type and p-type semiconductor materials, respectively; $V_{bi}$, the build-in potential; $V$, the applied voltage from p-side to n-side; and $q$ is the electronic charge. The similar equation is applied to the depletion width inside the p-type material.

The current–voltage ($I$–$V$) characteristic of a photodiode with no incident light is similar to a rectifying diode. When a reverse bias is applied, a small reverse current appears which is related to dark current $I_d$. When illuminating the photodiode with optical radiation, there is a shift of the $I$–$V$ curve by the amount of photocurrent. The measured current in photodiode $I_m$ is given by:

$$I_m = I_d - I_{ph} \tag{3}$$

where $I_d$ is the dark current; and $I_{ph}$ is the photocurrent.

A schematic energy band diagram of the n-ZnO nanowires/p-silicon structure and the working theory of the photodiode are illustrated in Fig. 2. When the photon energy of the incident light is higher than the bandgap of ZnO (3.3 eV, ~380 nm wavelength), electron–hole pairs are generated inside ZnO by light absorption. At the same time, the electron–hole pairs are separated by the electric field inside the depletion region of ZnO nanowires to generate the photocurrent. The light also generates electrons and holes in the neutral n-type and p-type regions, some of which can diffuse to the depletion layer, contributing to the photocurrent. In real devices, a barrier layer at the interface of ZnO nanowires/silicon could be present due to the very thin layer of native silicon dioxide that is not drawn in Fig. 2.

## 3. Fabrication

The fabrication process is illustrated in Fig. 3. First, naturally doped n-ZnO nanowires were synthesized on a p-silicon substrate with a doping level of $\sim 10^{18}\,cm^{-3}$ by the vapor transport method [15,16]. A thin layer of gold (30 Å) was deposited and used as the catalyst to initiate the growth of ZnO nanowires via the VLS growth mechanism. The substrate was placed inside a processing tube close to the source, which contained an equal amount of graphite/ZnO power, and then heated to 900 °C for the synthesis process under an argon gas flow of 20 standard cubic centimeters per minute (sccm). The growth rate of ZnO nanowires was approximately 1 μm/min and single-crystalline ZnO nanowires were synthesized as shown in Fig. 3(a). Due to the low formation energy of the oxygen vacancies and extra zinc interstitial atoms in the lattice during the synthesis process, ZnO nanowires show n-type characteristics. They can be further doped into n-type by introducing dopants, such as aluminum, gallium, indium or excess zinc, while p-type doping is much more difficult to achieve [17,18]. The nanowires were of 70–120 nm in diameter, and the length was 2–3 μm, although longer nanowires can be easily accomplished by controlling the growth time. Afterwards, a dielectric material, spin-on glass (SOG) was applied to provide insulation between nanowires and mechanical support for the upper electrode. The SOG layer was deposited onto the substrate using the spin-on process at the speed of 800 rpm twice to fully bury the ZnO nanowires. The device was then baked at 200 °C for 15 min for the solidification of SOG. Fig. 3(b) applies

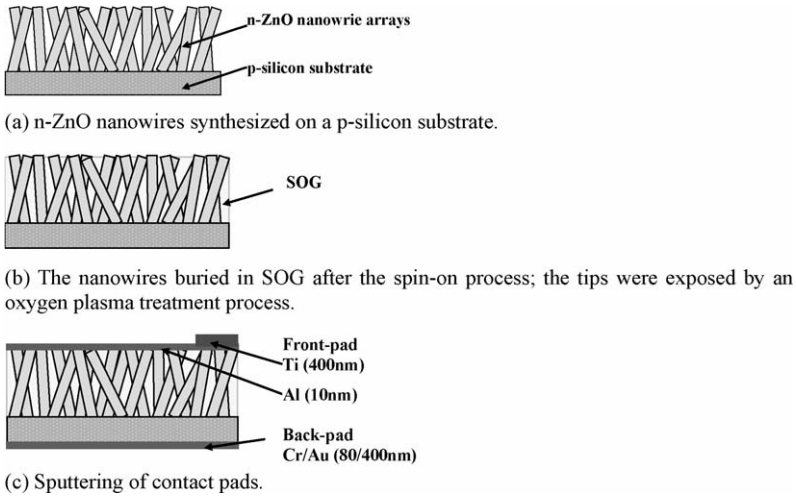


Fig. 3. Fabrication process for the n-ZnO nanowires/p-silicon photodiode. (a) n-ZnO nanowires synthesized on a p-silicon substrate. (b) The nanowires buried in SOG after the spin-on process; the tips were exposed by an oxygen plasma treatment process. (c) Sputtering of contact pads.

after these steps. After that, a 2-min oxygen plasma treatment at the power of 400 W was applied to remove some SOG that adhered to the tips of the nanowires. Finally, contact pads were sputtered onto the backside and front-side, respectively as illustrated in Fig. 3(c). Here, Cr/Au (80/400 nm) was deposited as the backside p-contact. A shallow, ∼10 nm-thick aluminum layer was deposited at the front side to maintain the transparency as well as to provide contacts to the individual nanowires. A 400 nm-thick titanium layer was deposited at the side as the contact pad. In this work, the top electrode area was defined by a circular shadow mask of about 1 mm in diameter using an aluminum foil as the masking material.

Fig. 4(a) shows the typical growth result of ZnO nanowires in the SEM microphoto after step (a) in Fig. 3. The growth direction of nanowires is not vertical to the substrate due to the different crystal structures and lattice mismatch of ZnO and silicon. Vertical growth can be achieved by using a substrate with the same crystal structure as ZnO, such as sapphire or SiC. A close view of the ZnO nanowires in Fig. 4(b) illustrates the hexagonal cross section of these nanowires. The high-resolution TEM image of a single-crystalline ZnO nanowire is shown in Fig. 5. The spacing between adjacent lattice planes corresponds to the distance between two (0 0 2) crystal planes, indicating the growth direction along the preferable ⟨0 0 1⟩ direction [15].

Using a low power nanosecond Nd:YAG laser (266 nm wavelength, 6–8 ns pulse duration and 10 Hz repetition rate) as the excitation source, we characterized the ZnO nanowire room temperature photoluminescence (PL) spectra. The pulsed laser beam excited the nanowires from a glance angle. As illustrated in Fig. 6, a strong near-band-edge emission and free-exciton peak centered at ∼385 nm dominated the PL spectra. Furthermore, no more emission band was found in scans at broader wavelength ranges, which is not shown here. All of these features indicate that the as-grown ZnO nanowires have good optical qualities. Fig. 7 is the SEM microphotos of the device after first and second SOG spin-on process. It shows the rigidity of nanowires during the spin-on process and that nanowires were fully buried after the second spin-on process.

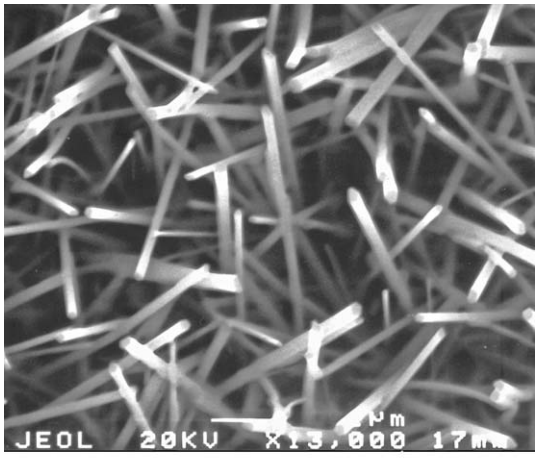


(a)

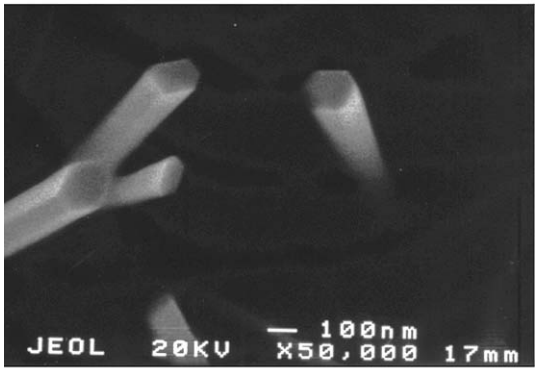


(b)

Fig. 4. SEM microphotos of ZnO nanowires. (a) SEM image of ZnO nanowires. (b) Close SEM image of the ZnO nanowires with hexagonal cross section.

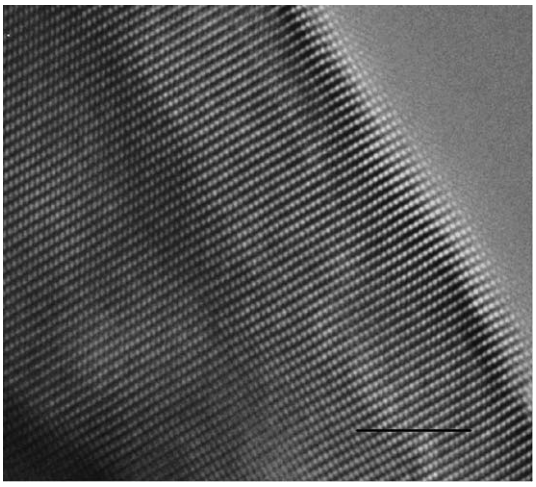

Fig. 5. TEM image of a single-crystalline ZnO nanowires with ⟨0 0 1⟩ growth direction. The scale bar is 3 nm.

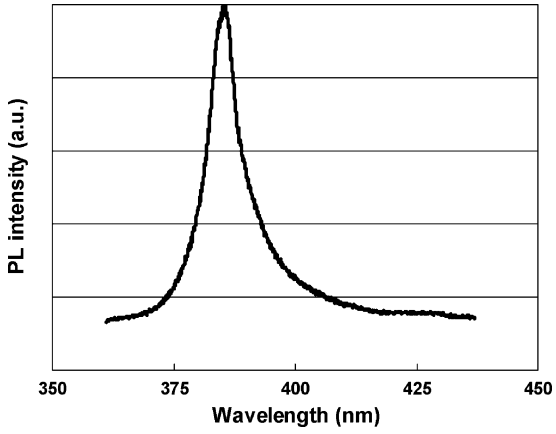


Fig. 6. Photoluminescence spectra of ZnO nanowires with a strong emission centered at ∼385 nm wavelength excited by 266 nm UV laser. (The photoluminescence intensity is in arbitrary unit, which is not shown.)

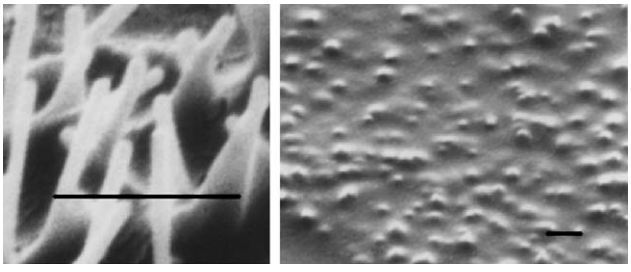

Fig. 7. SEM images of n-ZnO nanowires after first (left) and second (right) spin-on process. The scale bar in the pictures is 1 μm.

## 4. Experiment and results

Fig. 8 shows the current–voltage characteristics of the device measured in dark. The *I–V* relationship for a heterojunction is given by [13]:

$$I = I_S \left[ \exp\left( \frac{qV}{K_B T} \right) - 1 \right] \quad (4)$$

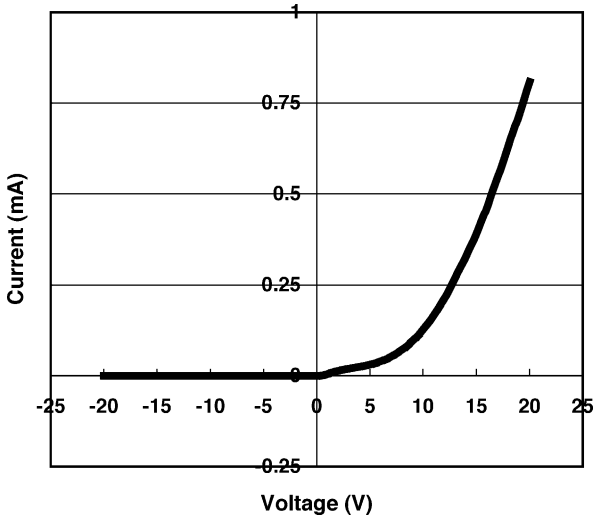


Fig. 8. *I–V* characteristics of the heterojunction in dark.

where $I$ is the current; $I_S$, the saturation current; $V$, the applied voltage across the heterojunction from p-side to n-side; $K_B$, the Boltzmann constant; and $T$ is the absolute temperate. The typical rectifying behavior of heterojunctions is observed in Fig. 8. Based on the SEM microphoto after the SOG spin-on process, the prototype device has about four nanowires per $\mu m^2$ on average to successfully form the heterojunction. Therefore, it is estimated that a total of about 2–3 millions nanowires contribute to the *I–V* measurements of the device that has an area of 1 mm in diameter.

The UV photoresponsivity measurement was performed using an Hg-lamp at the wavelength of 365 nm. Because the photon energy is higher than the bandgap of ZnO, UV light was absorbed by the ZnO nanowires creating electron–hole pairs, which were further separated by the electric field inside ZnO nanowires contributing to the increase of the external current. The penetration depth of UV light at 365 nm into ZnO was measured as ∼40 nm [6] that is less than the diameter of the ZnO nanowires synthesized in this work, thus, efficient light absorption is expected during experiments. In the experiments, reverse bias was used for the photodiode operation to maximize the depletion width, minimize the transit time, and the carrier loss due to the recombination process in diffusion region.

The photocurrent curves with reverse-biased voltage are recorded in Fig. 9. Under 25 μW UV (365 nm) illumination, the photodiode exhibits responsivity of ∼0.07 A/W at the 20 V reverse bias about 10 cm away from the light source. The responsivity $R$ is given by [13]:

$$R = \frac{I_{ph}}{P_{opt}} \quad (5)$$

where $I_{ph}$ is the photocurrent of the photodiode by the absorption of incident light; and $P_{opt}$ is the measured incident optical power at a wavelength $\lambda$.

The increase of the UV-driven photocurrent under reverse bias indicates the light absorption and photo-carrier gener-

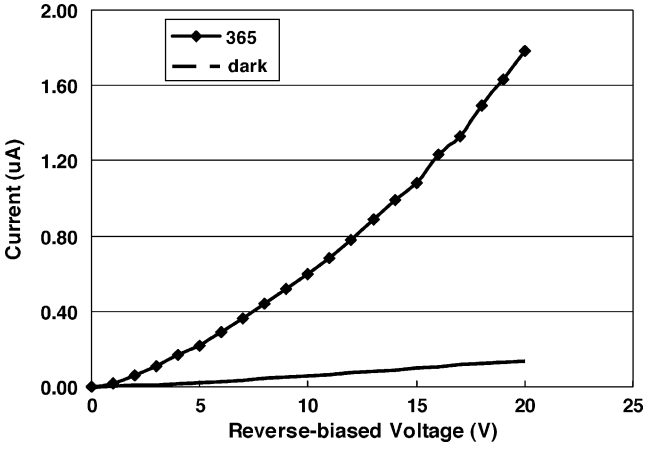


Fig. 9. Photocurrent curves of the n-ZnO nanowires/p-silicon photodiode with reverse-biased voltage under 25 μW UV illumination at 365 nm wavelength and in dark.

ation in ZnO nanowires. The photocurrent $I_{ph}$ is expressed as:

$$I_{ph} = Aq(\Delta n_{ph}\nu_n + \Delta p_{ph}\nu_p) \quad (6)$$

where $\Delta n_{ph}$ and $\Delta p_{ph}$ are the average electron and hole density generated by the UV light; and $\nu_n$ and $\nu_p$ are the average velocities of electrons and holes. Because the electric field strength inside the depletion region increases as the applied voltage increases, electrons and holes will have higher average velocities. As a result, the photocurrent increases with increased reverse bias, which is observed in Fig. 9. In reverse-biased mode, the carrier concentrations in depletion region are reduced below their equilibrium values, leading to the thermal generation of electrons and holes throughout the region. The generated carriers are swept rapidly into the quasi-neutral regions by the large electric field, adding to the dark current. Thus, the dark current never saturates, but continually increases with increasing reverse bias, which is also shown in Fig. 9.

The efficiency of the device is affected by several factors, including the existence of a thin native silicon dioxide barrier layer at the interface of the heterojunction that will reduce the photocurrent; the number of nanowires in good contact with the external circuit; possible small areas that are not covered by any nanowires; material defects of the nanowires and on the interface; and light loss by reflection and absorption of the top aluminum contact pad. Further investigations are needed to improve the device performance.

## 5. Conclusion

Using the bottom-up approach, we have successfully constructed a heterojunction of n-type ZnO nanowires and p-type silicon to demonstrate its applications in UV photodiodes. ZnO nanowires were synthesized via the VSL growth mechanism using a thin layer of gold as the catalyst. The performance of UV photodiodes could be enhanced due to the good UV responsivity and larger excitation area to volume ratio of ZnO nanowires. According to experimental results, the current–voltage characteristics of the device show the typical rectifying behavior of heterojunctions, and the photodiode exhibits response of ~0.07 A/W for UV light (365 nm) under a 20 V reverse bias. In summary, the prototype device provides a simple method for nano-material integration and also predicts the possibility of constructing nanoscale photodiodes for nano-optics applications. In the future, investigations such as using the front-side polishing and optimized post-annealing processes to get better external circuit contacts, and a higher transparent front-side contact pad to reduce the light loss could further improve the performance.

## Acknowledgements

The devices presented in this paper were fabricated in the Microlab at UC Berkeley and Lawrence Berkeley National Lab. The authors would like to thank Ron Wilson for taking the SEM photographs. Ms. Lei Luo is supported in part by an ITRI fellowship. This work is supported in part by NSF (ECS-041356) and DOE.

## References

[1] E. Monroy, F. Omnès, F. Calle, Wide-bandgap semiconductor ultraviolet photodetectors, Semicond. Sci. Tech. 18 (2003) R33–R51.
[2] N. Biyikli, O. Aytur, I. Kimukin, T. Tut, E. Ozbay, Solar-blind AlGaN-based Schottky photodiodes with low noise and high detectivity, Appl. Phys. Lett. 81 (2002) 3272–3274.
[3] M.L. Lee, J.K. Sheu, W.C. Lai, S.J. Chang, Y.K. Su, M.G. Chen, C.J. Kao, G.C. Chi, J.M. Tsai, GaN Schottky barrier photodetectors with a low-temperature GaN cap layer, Appl. Phys. Lett. 82 (2003) 2913–2915.
[4] A. Bouhdada, M. Hanzaz, F. Vigué, J.P. Faurie, Electrical and optical proprieties of photodiodes based on ZnSe material, Appl. Phys. Lett. 83 (2003) 171–173.
[5] S. Liang, H. Sheng, Y. Liu, Z. Huo, Y. Lu, H. Shen, ZnO Schottky ultraviolet photodetectors, J. Cryst. Growth 225 (2001) 110–113.
[6] I.-S. Jeong, J.H. Kim, S. Im, Ultraviolet-enhanced photodiode employing n-ZnO/p-Si structure, Appl. Phys. Lett. 83 (2003) 2946–2948.
[7] S.J. Pearton, D.P. Norton, K. Ip, Y.W. Heo, T. Steiner, Recent advances in processing of ZnO, J. Vac. Sci. Technol. B 22 (2004) 932–948.
[8] Y. Cui, C.M. Lieber, Functional nanoscale electronic devices assembled using silicon nanowire building blocks, Science 291 (2001) 851–853.
[9] R. Martel, T. Schmidt, H.R. Shea, T. Hertel, Ph. Avouris, Single- and multi-wall carbon nanotube field-effect transistors, Appl. Phys. Lett. 73 (1998) 2447–2449.
[10] M.S. Gudiksen, L.J. Lauhon, J. Wang, D.C. Smith, C.M. Lieber, Growth of nanowire superlattice structures for nanoscale photonics and electronics, Nature 415 (2002) 617–620.
[11] A. Star, Y. Lu, K. Bradley, G. Gruner, Nanotube optoelectronic memory devices, Nano. Lett. 4 (2004) 1587–1591.

[12] L. Luo, Y. Zhang, S.S. Mao, L. Lin, ZnO nanowires based UV photodiodes, in: Proceedings of 18th IEEE MEMS Conference, Miami, 2005, pp. 427–430.
[13] S.M. Sze, Physics of Semiconductor Devices, second ed., Wiley, New York, 1981.
[14] A.G. Milnes, D.L. Feucht, Heterojunctions and Metal-Semiconductor Junctions, Academic Press, New York, London, 1972.
[15] M.H. Huang, Y. Wu, H. Feick, N. Tran, E. Weber, P. Yang, Catalytic growth of zinc oxide nanowires by vapor transport, Adv. Mater. 13 (2001) 113–116.
[16] J. Park, H. Choi, Y. Choi, S. Sohn, J. Park, Ultrawide ZnO nanosheets, J. Mater. Chem. 14 (2004) 35–36.
[17] D.P. Norton, Y.W. Heo, M.P. Ivill, K. Ip, S.J. Pearton, M.F. Chisholm, T. Steiner, ZnO: growth, doping & processing, Mater. Today (2004) 34–40.
[18] C.H. Park, S.B. Zhang, S. Wei, Origin of *p*-type doping difficulty in ZnO: The impurity perspective, Phys. Rev. B 66 (2002) 073202.

## Biographies

**Lei Luo** received her BS in Department of Precision Instruments from Tsinghua University, P.R. China, in 2002. She is currently working towards her PhD degree in the field of nano- and micro-systems at the University of California at Berkeley. Her research interests include nano-electronic and optoelectronic devices, nano-material integrations and microelectromechanical systems.

**Yanfeng Zhang** is a scientific staff member of Lawrence Berkeley National Laboratory's Advanced Energy Technologies Department. He obtained his PhD degree from the Chinese Academy of Science in 2000. Before joining LBNL in 2004, he was a visiting researcher of the University of California at Berkeley from 2002 to 2003, a postdoctoral researcher of Yale University from 2001 to 2002, and a visiting scholar of the Hong Kong University of Science and Technology from 2000 to 2001. Dr. Zhang's primary research interest is the development of one-dimensional nanoscale materials and optoelectronic devices. He has published 15 refereed scientific articles in the fields of optoelectronics and nanotechnology.

**Samuel S. Mao** is a staff scientist and leader of nanotechnology team of the Advanced Energy Technologies Department, Lawrence Berkeley National Laboratory (LBNL). He joined LBNL after receiving his PhD degree in 2000 from the Mechanical Engineering Department of the University of California at Berkeley. Since 2004, he became an assistant adjunct professor of mechanical engineering of the University of California at Berkeley. Dr. Mao's research interests include fabrication and characterization of nanostructured materials and nanoscale optoelectronic devices, ultrafast laser engineering, and the application of nanotechnology for energy efficiency. He currently serves in the judging panel of R&D 100 Awards and in the SPIE's laser applications in microelectronic and optoelectronic manufacturing program committee. He is the associate editor of International Journal of Nanotechnology.

**Liwei Lin** received his BS degree from National Tsing-Hua University, Taiwan in 1986 and the MS and PhD degrees in mechanical engineering from the University of California, Berkeley, in 1991 and 1993, respectively. He joined BEI Electronics Inc. USA from 1993 to 1994 in microsensors research and development. He was an associate professor in the Institute of Applied Mechanics, National Taiwan University, Taiwan from 1994 to 1996 and an assistant professor at the Mechanical Engineering Department at the University of Michigan from 1996 to 1999. He joined the University of California at Berkeley in 1999 and is now a professor at Mechanical Engineering Department and co-director at Berkeley Sensor and Actuator Center, NSF/Industry/University Research Cooperative Center. His research interests are in design, modeling and fabrication of micro/nano structures, micro/nano sensors and micro/nano actuators as well as mechanical issues in micro/nano electromechanical systems and he holds eight U.S. patents. Dr. Lin is the recipient of the 1998 NSF CAREER Award for research in MEMS Packaging and the 1999 ASME Journal of Heat Transfer best paper award for his work on micro scale bubble formation. He is a subject editor for IEEE/ASME Journal of Microelectromechanical Systems and North and South America Editor for Sensors and Actuators – A Physical. He has been the founding chairman of the ASME MEMS division since 2004.